We are IntechOpen,
the world's leading publisher of
Open Access books
Built by scientists, for scientists

3,900
Open access books available

116,000
International authors and editors

120M
Downloads

154
Countries delivered to

Our authors are among the

TOP 1%
most cited scientists

12.2%
Contributors from top 500 universities

WEB OF SCIENCE™

Selection of our books indexed in the Book Citation Index
in Web of Science™ Core Collection (BKCI)

Interested in publishing with us?
Contact book.department@intechopen.com

Numbers displayed above are based on latest data collected.
For more information visit www.intechopen.com

Time Resolved Investigation of Fast Phase-Change Phenomena in Rewritable Optical Recording Media

Shigeru Kimura[1], Yoshihito Tanaka[1,2], Shinji Kohara[1] and Masaki Takata[1,2,3]
[1]Research & Utilization Division, Japan Synchrotron Radiation Research Institute
[2]RIKEN SPring-8 Center, RIKEN Harima Institute
[3]School of Frontier Science, The University of Tokyo
Japan

1. Introduction

The worldwide hunger for secure and smarter electronic data storage grows daily to satisfy today's extremely demanding business and entertainment requirements, and this drives the need to pack data into an increasingly smaller volume at ever faster speeds. Digital versatile disks (DVDs) are one of the most convenient storage devices for large amount of information such as video and digital graphs. One of the keys to develop the DVDs was to create the fast phase-change material, which gives rise to faster bi-directional phase change between crystal phase and amorphous phase by laser heating within the recording mark. Another key was to minimize the size of the recording mark for high density data storage. The DVDs have already been a mass product as one of the indispensable home electronic appliances, even though the mechanism of fast phase change has been the remained problem to be solved. Then, to develop the next generation higher density and faster optical data storage system, the atomic and electron level study was required in the last decades. This chapter will describe the challenge of the atomic level research for the fast phase-change mechanism of the DVD materials via X-ray pinpoint structural measurement, which is the state-of-the-art synchrotron radiation (SR) materials-analysis techniques developed at SPring-8. The X-ray pinpoint structural measurement and it's data analysis technique has been further upgraded by combining with theoretical structure modelling and became a tool to investigate how laser pulses alter the atomic structure of a class of materials useful for data storage and uncover a mechanism that could help the development of even faster information storage in the future.

So far, the great efforts and developments have been paid for the progress of the DVD materials (Wutting & Yamada, 2007). The development of new phase-change materials, leading to the discovery of GeTe-Sb_2Te_3 (Yamada et al., 1987) and of $Ag_{11}In_{11}Sb_{55}Te_{23}$ (Iwasaki et al., 1992), has allowed us to produce rewritable compact discs, DVDs, and Blu-ray discs. In the commercial rewritable DVDs such as DVD-random access memory (RAM) and DVD-rewriteable (RW), information is written to the phase-change materials composed of the alloys of Ge, Sb and Te, or those of Ag, In, Sb and Te by changing their phase locally between amorphous and crystalline states using a sub-micrometer sized laser irradiation.

The recording and erasing are performed by controlling the laser intensity for irradiation, yielding a difference in the transient heating and cooling rates of the materials. A higher cooling rate from a temperature above the melting point generates the amorphous phase; a lower rate produces the crystalline phase from the amorphous phase. Because the optical reflectivity of the two states is different, this information can be easily read from the disk by measuring the reflectance with a low power laser. Recently developed DVD materials can complete the phase change with a 20 ns laser irradiation (Fig. 1).
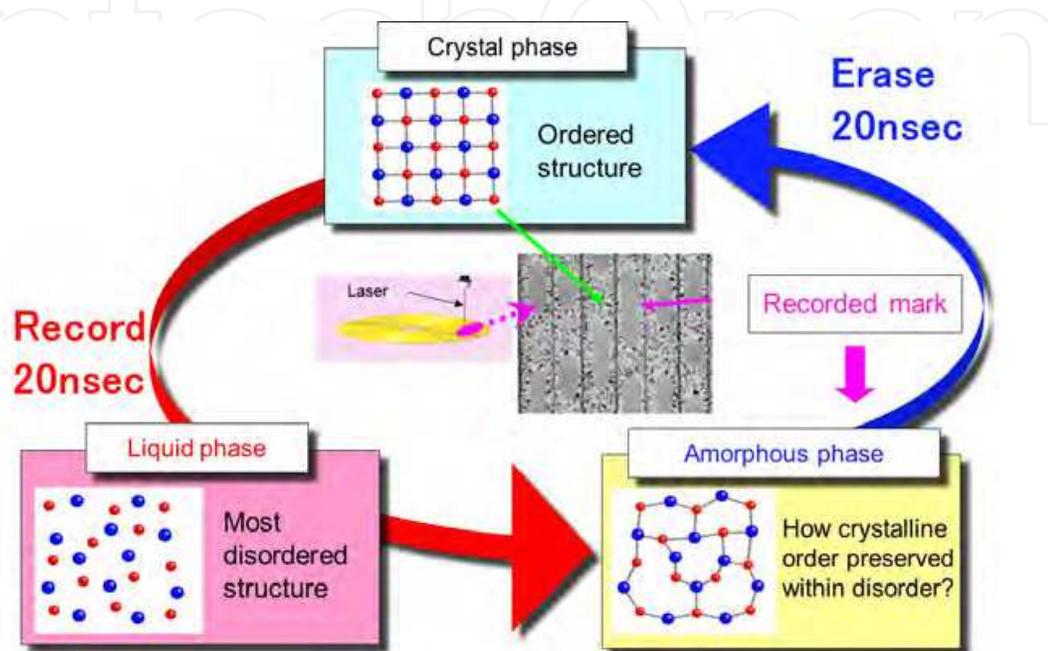

Fig. 1. Schematic illustration of recording and erasing process in rapid phase-change materials.

In contrast to the reliability and high-speed-performance of DVD media, the mechanism of rapid phase change, especially crystallization from the amorphous phase is still not fully understood, in spite of a lot of investigation using transmission electron microscopy (Park et al., 1999; Naito et al., 2004), fluctuation electron microscopy (Kwon et al., 2007), optical (Wei & Gan, 2003), electronic (Lee et al., 2005), and structural (Yamada & Matsunaga, 2000; Kolobov et al., 2004; Kohara et al., 2006) studies. We therefore developed the X-ray pinpoint structural measurement system (Kimura et al., 2006), which enables the 40 picosecond time resolved pump and probe X-ray diffraction experiment using 100 nm scale SR beam. Using the system, we achieved the real-time *in situ* structural observation of the amorphous-crystal phase change process in nanosecond time-scale (Fukuyama et al., 2008a). The obtained results using the time-resolved X-ray diffraction apparatus coupled with *in situ* optical reflectivity monitor showed the strong correlation between the crystal growth and optical reflectivity, and the difference in the crystal growth process between $Ge_2Sb_2Te_5$ (GST) and $Ag_{3.5}In_{3.8}Sb_{75.0}Te_{17.7}$ (AIST).

In the following section, we describe the detail of the X-ray pinpoint structural measurement system for investigation of optical recording process and its performance (Tanaka et al., 2009). Moreover, we describe the recent progress for fully understanding the atomic structure of AIST and compare it to GST through the research with X-ray diffraction,

extended X-ray absorption fine structure (EXAFS), hard X-ray photoelectron spectroscopy (HXPS) measurements and computer simulations (Matsunaga et al., 2011).

2. X-ray pinpoint structural measurement system for investigation of optical recording process

The pulse characteristic and high coherent X-ray beam of SPring-8 allow us to investigate dynamics of chemical reactions and phase transition of materials caused by applied field. In order to realize the direct investigation, we developed the X-ray pinpoint structural measurement system at BL40XU of SPring-8, which enables the advanced X-ray measurement technique in nanometer spatial scale and/or picosecond time scale. This system was used not only for investigation of optical recording process but also for charge density level visualization of photo-induced phase transition (Fukuyama et al., 2010) and sub-micron single crystal structure analysis (Yasuda et al., 2008; Yasuda et al., 2010).

In order to investigate the amorphous-crystal phase change on recording DVD media we optimized the X-ray pinpoint structural measurement system. Figure 2 shows the schematic illustration of experimental setup for taking a snapshot of X-ray diffraction profile of optical phase-change materials. The main optimized components are laser-SR timing control system, a sample rotation system, an optical reflectivity probe system, and an X-ray diffractometer. The following sub-sections describe the components and their performance.
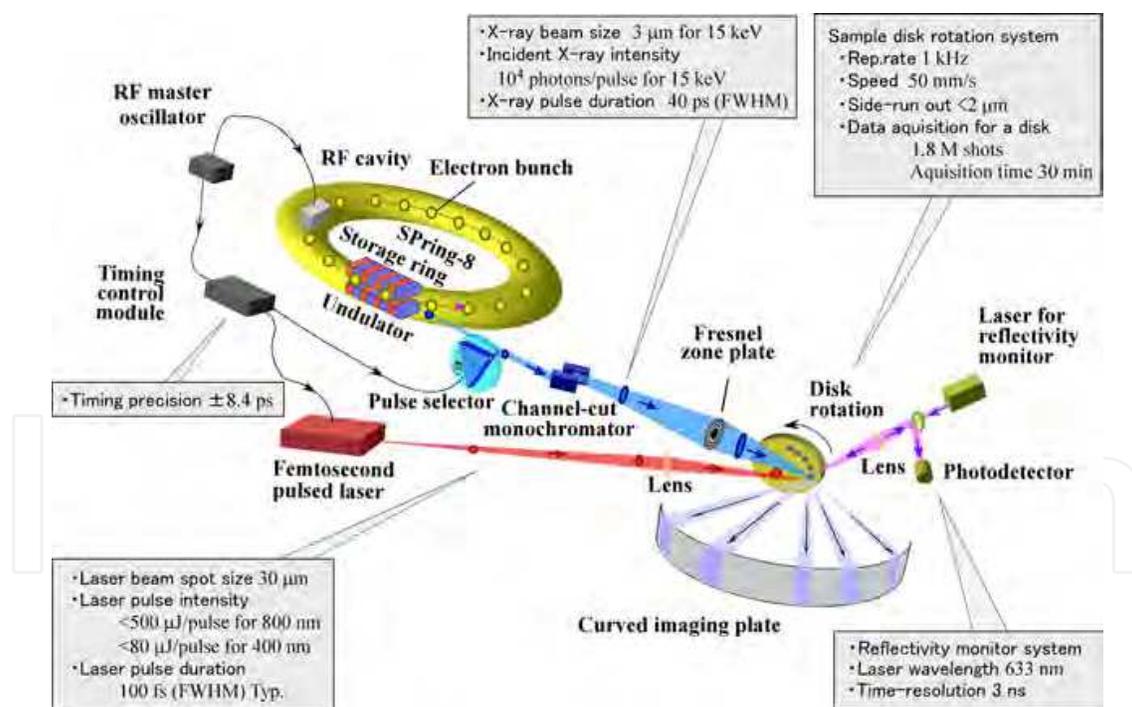

Fig. 2. Experimental setup for taking a snapshot of X-ray diffraction profile of optical phase-change materials.

2.1 Laser-pump and X-ray SR probe system

A pulsed nature of synchrotron X-ray beam due to the acceleration mechanism of charged particles has enabled us to conduct the stroboscopic X-ray measurement in picosecond time-

scale. In the stroboscopic X-ray diffraction measurement, the pulsed X-rays from a SR source are diffracted at a sample after a short-pulsed laser synchronized to the SR X-ray pulses illuminates it, as schematically shown in Fig. 3. The time-dependent snapshot can be taken by changing the time delay indicated as τ in Fig. 3.
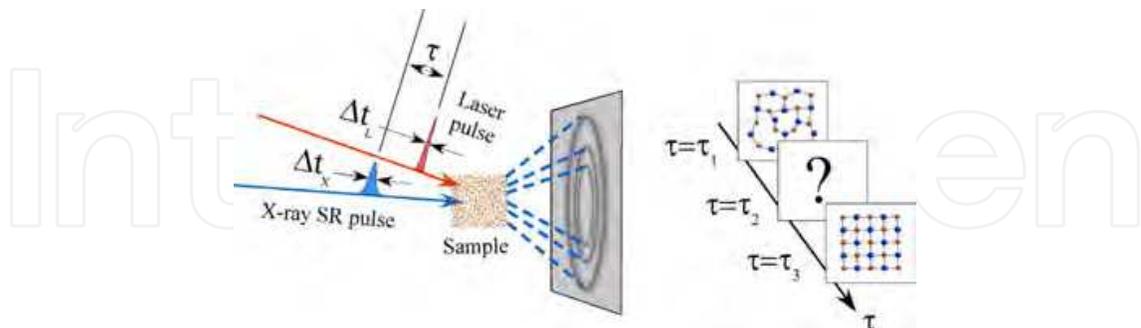

Fig. 3. Schematic illustration of time-resolved X-ray diffraction measurement using a laser-pump X-ray-probe method.

To measure an impulse response of the crystallization, a mode-locked Ti:sapphire laser with a pulse width, Δt_L, of 130 fs was used as a pump laser. A photo of the laser system is shown in Fig. 4. The laser system is equipped with a regenerative amplifier which produces pulses with a pulse energy of 1 mJ, a wavelength of 800 nm, and a repetition rate of 1 kHz. The laser was synchronized to the RF master oscillator of the SR storage ring for acceleration of electrons, as shown in Fig. 2. Since the detailed synchronization system was published (Tanaka et al., 2000), the synchronization and timing control system are briefly summarized here. Timing synchronization of the mode-locked laser oscillator was achieved by controlling the cavity length, with the precision of a few ps. The repetition rate is 84.76 MHz, corresponding to the 1/6 of RF of the storage ring master oscillator. Output timing of regeneratively amplified laser pulses is controlled in consideration of the revolving frequency (the round trip is ~5 µs) of the storage ring.
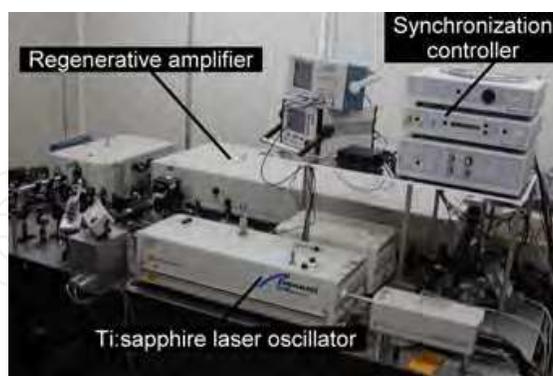

Fig. 4. Femtosecond pulsed laser system. The laser system is mainly composed of a Ti:sapphire laser oscillator and a regenerative amplifier. The regenerative amplifier produces optical pulses with a pulse energy of 1 mJ, a wavelength of 800 nm, and a repetition rate of 1 kHz.

Figure 5 shows a time chart of the laser and the SR pulses in the experiment. The time structure of SR pulses is dependent on the filling pattern of electron bunches in the storage ring. Because the repetition rate of the measurement was ~1 kHz, only one bunch in the

storage ring was used for the measurement. The filling pattern was set to be hybrid mode, in which the high current electron bunch (3 mA) exists with lower current bunch train (see Fig. 5(a)). In the filling pattern, the pulse width of SR, which is determined by the electron bunch length was ~40 ps (FWHM).
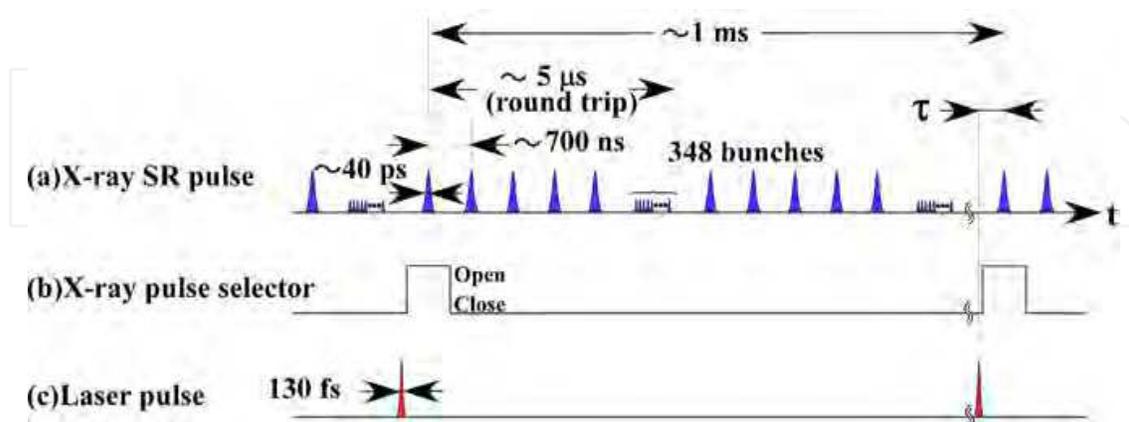

Fig. 5. Time chart of the pulsed laser and X-ray SR irradiation for a snapshot measurement with a time delay of τ.

The control technique of the timing delay, τ, is also a key to make a stroboscopic measurement. As the time-scale of completing the phase change is a microsecond, the large delay is required, which is generally difficult to obtain with an optical delay. Thus, we developed a high precision RF phase control delay circuit to scan the time delay without degrading the precision (Fukuyama et al., 2008b). Figure 6 shows the photograph of the RF phase control circuit, whose timing jitter between the output and the input RF signal is about 3 ps (in rms), which was evaluated with a 16 GHz digital oscilloscope (Tanaka et al., 2010). The timing control precision in the whole system was 8.4 ps (in rms), which was estimated by time-resolved diffraction measurement using a fast lattice response of semiconductor single crystal. Since the distribution of the crossing points is narrower than the pulse width of the SR, the pump-probe system has a time resolution of < 40 ps.

Fig. 6. High precision RF phase control circuit. The circuit provides a delayed RF signal from the output port with a precision of better than 3 ps (in rms) which is independent of the delay time.

2.2 Rotating stage for sample holder

Repetitive measurement is necessary when the diffraction intensity for one shot was too low to obtain the profiles with high time resolution. Therefore the sample was rotated to give a virgin sample for every measurement, as shown in Fig. 2. To perform 1 kHz-repetitive measurement, the rotation speed of the disk and the laser beam size on the sample are adjusted to satisfy the requirement of v (m/s) > f (Hz) · s (m), where the v, f, and s are the moving speed of the disk, the repetition rate, and a beam diameter of the laser or X-rays, respectively. In addition, an X-ray microbeam technique with a phase zone plate was applied to achieve a few micron X-ray beam size, since the smaller beam gives a larger number of data for one disk. The laser beam diameter on the sample was adjusted to be about 30 μm in the moving direction with a 40 mm-focal lens. The parameters in the experiment are summarized in Table 1, together with the parameters for 5 Hz-measurement without X-ray microbeam (Fukuyama et al., 2008a) for comparison.

Repetition rate (Hz)	Disk rotation speed (m/s)	Laser beam size (μm)	X-ray beam size (μm)	Number of repetition for one disk
1×10^3	8×10^{-2}	30	3	1.8×10^6
5	5×10^{-3}	300	50	3×10^4

Table 1. Optical parameters of the time-resolved X-ray diffraction measurement system.

Figure 7 shows the photograph of the DVD sample attached on a rotating stage. The measurement with high repetition rate using microbeams enabled us to obtain a diffraction intensity profile within an hour for one disk sample, and to get systematic data.
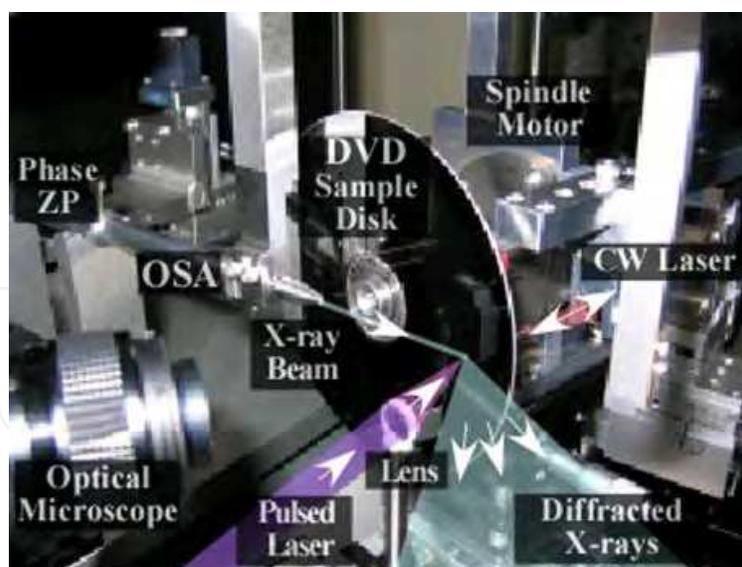

Fig. 7. Photograph around the sample disk.

2.3 Optical reflectivity measurement system

On-line monitor system of the time profile of optical reflectivity was installed to check the phase-change condition of the DVD sample. As shown in Fig. 7, a He-Ne laser beam was guided through the transparent substrate onto the backside of the sample, since the

clearance is too small on the right side due to a relatively shorter working distance of the lens for the pump laser. The reflected light intensity was monitored through a beam splitter with a photodiode having a response time of 10 ns, and the signal was stored in a digital oscilloscope.

2.4 High-precision X-ray diffractometer

The intense X-ray beam produced from an undulator is guided to the sample through a double curved mirror system, a pulse selector (rotating shutter), a Si(111) channel-cut monochromator, and a high-precision diffractometer with a phase zone plate (ZP) focusing system (Yasuda et al., 2008), as shown in Fig. 8. The ZP has the diameter of 100 µm, the innermost zone radius of 5.0 µm, the outermost zone width of 250 nm, and the tantalum thickness of 2.5 µm. The photon energy, E, and energy resolution, $\Delta E/E$, tuned by the channel-cut monochromator, were 15 keV, and ~10^{-4}, respectively. The X-ray beam was focused by the ZP, and the 1st order focused beam is only selected with the order sorting aperture placed in front of the sample position. The beam size at the sample position was ~3 µm, evaluated by a knife edge scan method using Au meshes. The focused beam intensity for one pulse at the sample position was ~10^4 photons/pulse, which is ~10^{-11} of the number of photons for a second in the upstream of the pulse selector. As described in Table 1, the total number of photons incident on the sample are then estimated to be ~10^{10} photons for one sample disk.
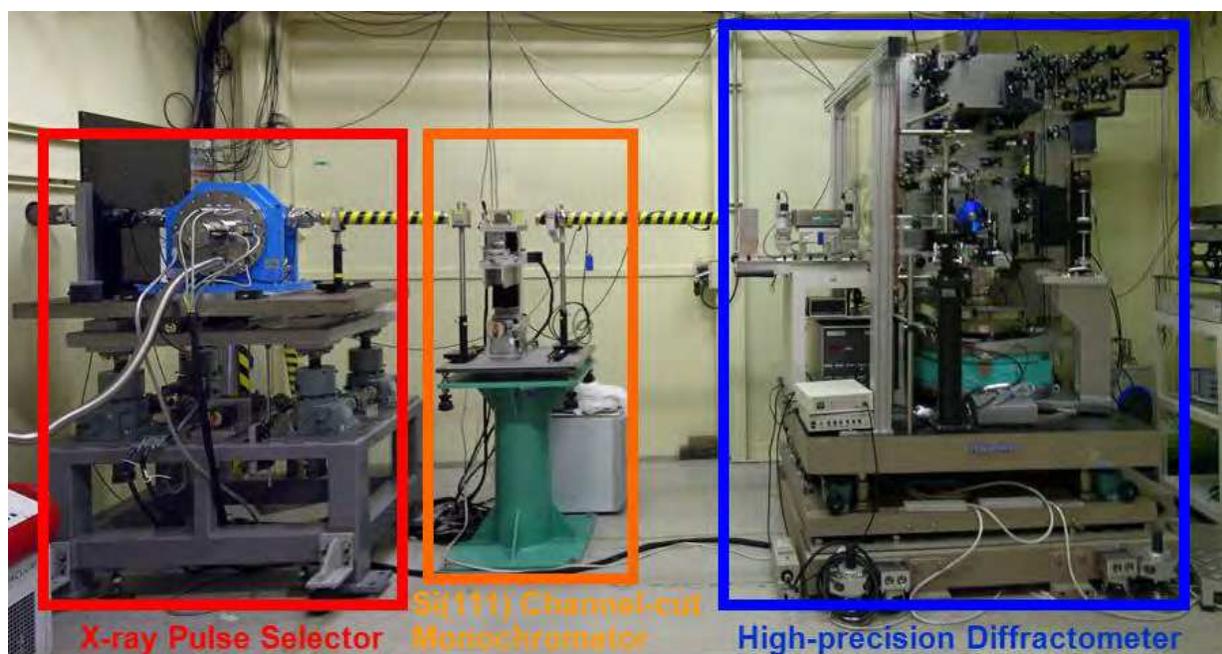

Fig. 8. Photograph of the X-ray pulse selector, the Si(111) channel-cut monochromator and the high-precision diffractometer.

A curved imaging plate (IP) was employed to obtain an X-ray diffraction profile. The use of an IP is advantageous in such longer exposure time as ~30 min in the present experiment. To obtain one-dimensional diffraction profile, the signal intensity was integrated using the full area of IP to compensate the smaller number of incident photons on the sample.

2.5 Performance of the X-ray pinpoint structural measurement system for investigation of optical recording process

Here we briefly summarize the X-ray pinpoint structural measurement system for investigation of optical recording process (see Fig. 2). The time-resolution and time precision are ~40 ps and ±8.4 ps, respectively. The spatial resolution is determined by the area of the laser beam of 30 μm, which is larger than the X-ray beam size of 3 μm. The maximum repetition rate is 1 kHz, in which the fresh sample area on the rotating disk appears at the irradiating position for every measurement. All parameters shown here are described in full width at half maximum.

3. Time-resolved investigation of nanosecond crystal growth in rapid-phase-change materials

Using the X-ray pinpoint structural measurement system described in previous section, we investigated the crystallization process of GST and AIST (Fukuyama et al., 2008a), which are thought to exhibit different crystallization behavior. To reveal the crystallization process of the amorphous phase in these rapid-phase-change materials, it is necessary to know (i) the time constants of both crystallization and optical reflectivity changes, and (ii) crystallization behavior. We therefore employed avalanche photodiode (APD)/multi-channel scaling (MCS) measurement with a time resolution of 3.2 ns coupled with optical reflectivity measurement for (i) and imaging plate (IP)/pump-probe measurement of a time resolution of 40 ps for (ii) as schematically shown in Fig. 9(a). Figure 9(b) shows the experimental method and the time chart for pump-probe measurement using 40 ps X-ray pulses and synchronous femtosecond laser pulses. The DVD samples were prepared by depositing GST and AIST on a SiO_2 glass substrate (12 cm diameter and 0.6 mm thick) with a 2-nm-thick 80 mol% ZnS-20 mol% SiO_2 cap layer. The thickness of the sample was 300 nm, which gave sufficient X-ray diffraction intensities for structure characterization and sufficient stability of the amorphous phase to avoid spontaneous crystallization.
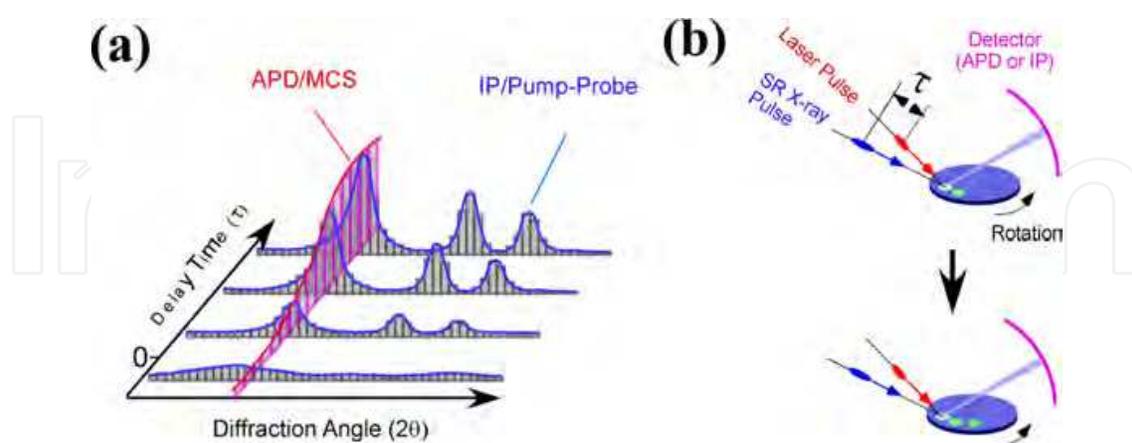

Fig. 9. (a) Schematic diagram of APD/MCS and IP/pump-probe measurement and (b) scheme of DVD rotating system and the time chart of pump-probe measurement.

Figure 10 shows the time-profiles of the X-ray diffraction intensity of Bragg peaks (black and blue lines) together with those of the optical reflectivity profiles (red lines) of (a) GST and (b) AIST, respectively, measured by APD/MCS measurement. These show good

accordance, which prove the close relation between the X-ray diffraction intensity and the optical reflectivity of the phase-change materials, *i.e.*, the structure and the electronic properties.
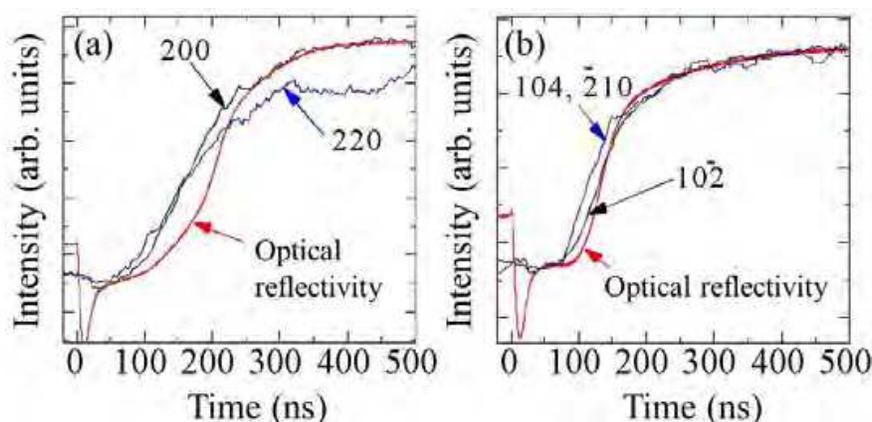

Fig. 10. Time-evolution of the optical reflectivity and X-ray diffraction intensity of (a) GST and (b) AIST.

From the intensity profile measured by the APD/MCS method, the delay times, τ, were determined for the IP/pump-probe method. Figure 11(a) shows the diffraction patterns obtained from the IP/pump-probe method for a 40 ps snapshot. Since the intensity of each diffraction peak has a uniform time-dependent increase, there is no crystal-crystal phase transition in GST and AIST during the crystal growth. We estimated the grain sizes from the line width of Bragg reflection, as shown in Fig. 11(b). In GST, the grain size is nearly constant (=70 nm), while the grain size significantly increases up to 1 µs in AIST. It is remarkable that the volume fraction of the crystal phase is almost saturated at 300 ns (see Fig. 10). Thus these observations suggest the coalescence of the crystal domains after 300 ns.
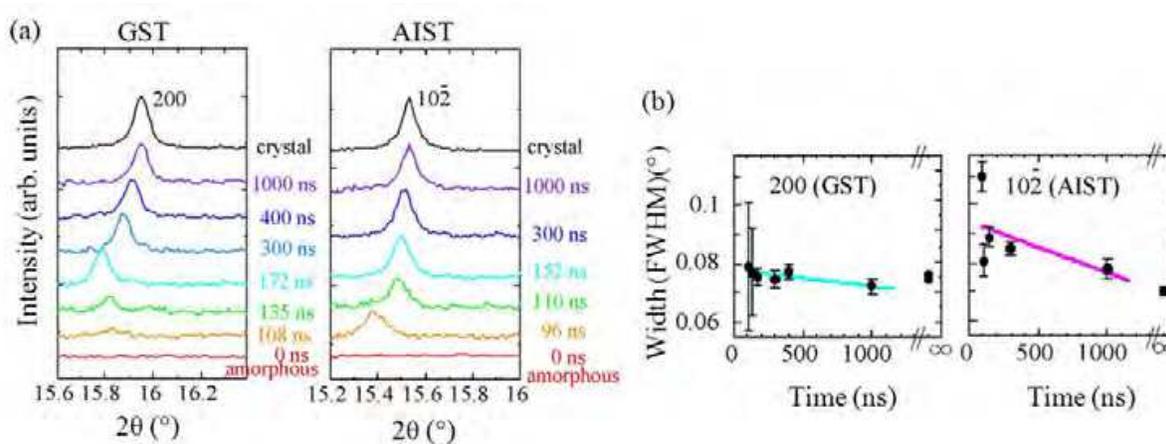
Fig. 11. (a) Snapshots of X-ray diffraction patterns and (b) the changes in peak width.

From the above experimental findings, we propose schematic models for the crystallization processes of GST and AIST as shown in Fig. 12. In the case of GST, nucleation takes place in the whole area in the amorphous phase after laser irradiation (A), and the number of newly formed crystallites of 70 nm diameter increases during the cooling process until 300 ns (B-

C). The crystal growth is then disturbed by the impingement of crystallites with each other (D). Our schematic model is consistent with the nucleation-driven crystallization process (Zaou et al., 2000).
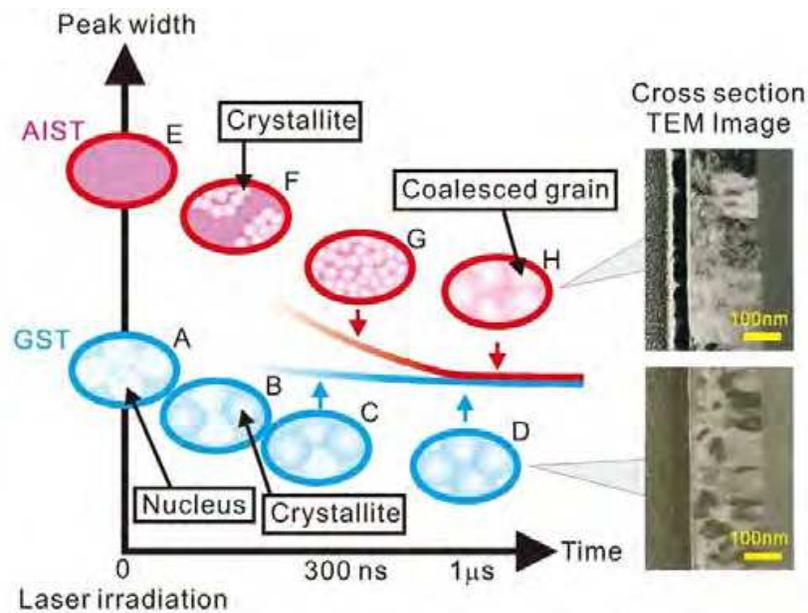

Fig. 12. (a) Schematic models with TEM image for the crystallization processes in GST and AIST.

On the other hand, the nuclei of AIST can immediately transform to smaller crystallites (<< 60 nm), which form domains (F). These domains are enlarged by edge-growth crystallization (F-G) and the crystallites coalesce at the final stage (300 ns~) of crystallization in AIST (G-H). These proposed schematic models are consistent with the TEM pictures, in which GST has a grainy texture filled with 100-nm-size grains, whereas AIST has a fine texture.

4. Nanosecond recrystallization dynamics in GST and AIST

To uncover recrystallization dynamics in GST and AIST at atomic level, we investigated the atomic structure of the amorphous phase by using a combination of advanced synchrotron radiation measurements (X-ray diffraction, EXAFS, HXPS) and reverse Monte Carlo simulation (RMC)/density function theory (DF)-molecular dynamics (MD) simulations (Matsunaga et al., 2011).

Figure 13 shows the structure factors $S(Q)$ of AIST and GST obtained using X-ray diffraction. The crystalline forms of both materials have sharp Bragg peaks (red lines), and the amorphous forms (blue lines) have typical halo patterns. However, oscillations up to the maximum Q value in a-AIST indicate a structure with well defined short-range order. The total correlation functions $T(r)$ for AIST and GST are shown in Fig. 14. The $T(r)$ for crystalline (c-) AIST and c-GST, which are very similar beyond 4 Å. Small differences between the two crystalline forms are found at shorter distances, for example the double peak in c-AIST (2.93 Å and 3.30 Å) and a single peak in c-GST (2.97 Å). The $T(r)$ for the amorphous materials, however, are significantly different: the first peak in amorphous (a-)

AIST (2.86 Å) is only slightly shorter than that found in c-AIST (2.93 Å), whereas the first peak in a-GST (2.79 Å) is shorter than that in c-GST (2.97 Å). We note also that the shoulder on the second peak in a-AIST (3.50 Å) is near that observed in the crystalline form (3.30 Å). The pronounced difference between the diffraction patterns of the two materials is strong evidence that they crystallize differently. The atomic motion and/or diffusion accompanying the phase change are larger in GST than in AIST, where the phase change is accompanied by small changes in bond lengths.
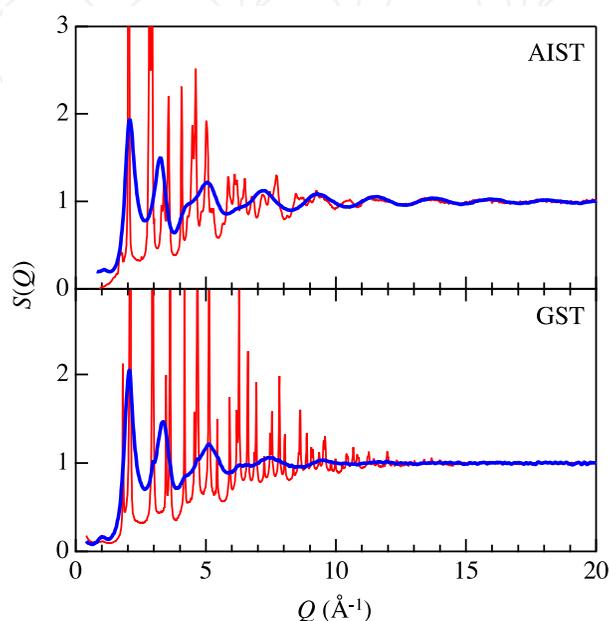
Fig. 13. Total structure factors, $S(Q)$, for AIST and GST. Blue line, amorphous form; red line, crystalline form.
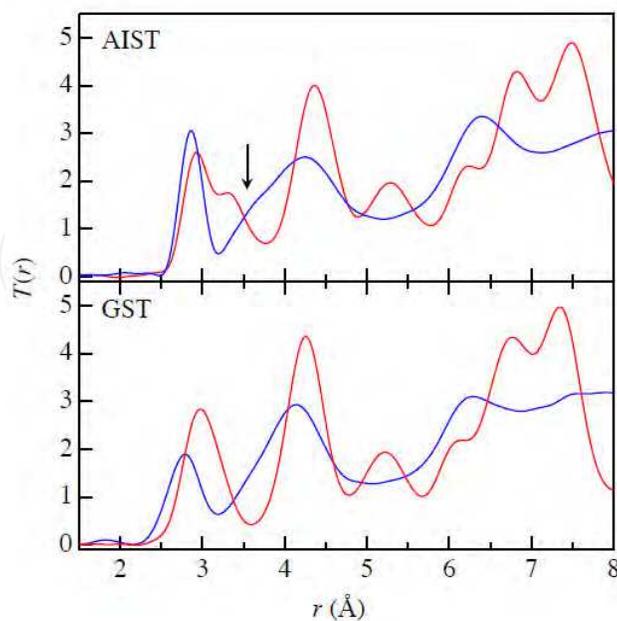
Fig. 14. Total correlation functions, $T(r)$, for AIST and GST. Blue line, amorphous form; red line, crystalline form.

Atomic configurations for a-AIST and a-GST obtained from the RMC / DF-MD simulations are shown in Fig. 15. It is found from the atomic configurations that the local environment of the predominant element Sb (75%) is very similar to that in the crystal (A7, a distorted octahedron) in AIST whereas large fraction of ABAB squares (manifested by ring) is observed in a-GST.
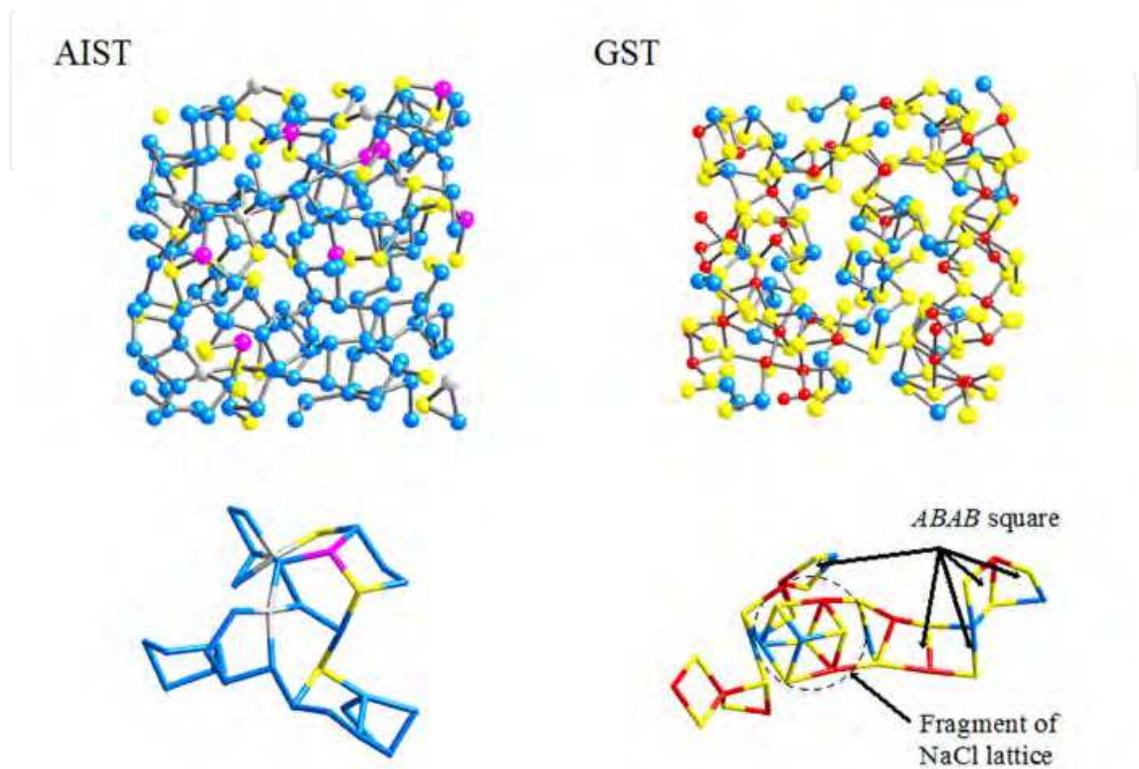

Fig. 15. Atomic configurations for a-AIST and a-GST obtained from the RMC / DF-MD simulations. Ag, silver; In, magenta; Sb, blue; Te, yellow; Ge, red.

Figure 16(a) shows ring statistics in a-AIST and a-GST derived from the RMC/DF-MD models which are consistent with the results of X-ray diffraction, EXAFS and HXPS measurements. In a-GST, 40% of the rings are fourfold or sixfold, whereas the distribution in a-AIST is much broader; the most common (fivefold) rings make up only 15% of the total. On the basis of structural features mentioned above, possible phase-change schemes in both materials are shown in Fig. 16(b). In a-AIST, it is suggested that a sequence of ring reconstructions by way of bond interchanges results in sixfold rings with short Sb bonds accompanied by small changes in the bond lengths, because RMC/DF-MD model for a-AIST has locally distorted 3+3 octahedron, which resembles c-AIST. By contrast, many four- and sixfold rings in a-GST act as nuclei for crystallization and require larger atomic displacements than in a-AIST. Crystallization starts simultaneously from many such nuclei in the amorphous mark (NaCl fragments) and lead to an aggregation of small crystal grains. These features propose a "bond-interchange" model as the origin of "growth-dominated" crystallization of a-AIST, whereas the large fraction of "crystalline nuclei" in a-GST is the origin of the "nucleation-driven" crystallization in GST. The structural finding and possible phase-change mechanism at atomic level obtained in this study is in line with the results of

time resolved measurements mentioned above. A combination of advanced synchrotron measurements and computer simulation has provided insight into the atomistic differences between two phase-change materials, which is related to their different crystallization mechanisms.
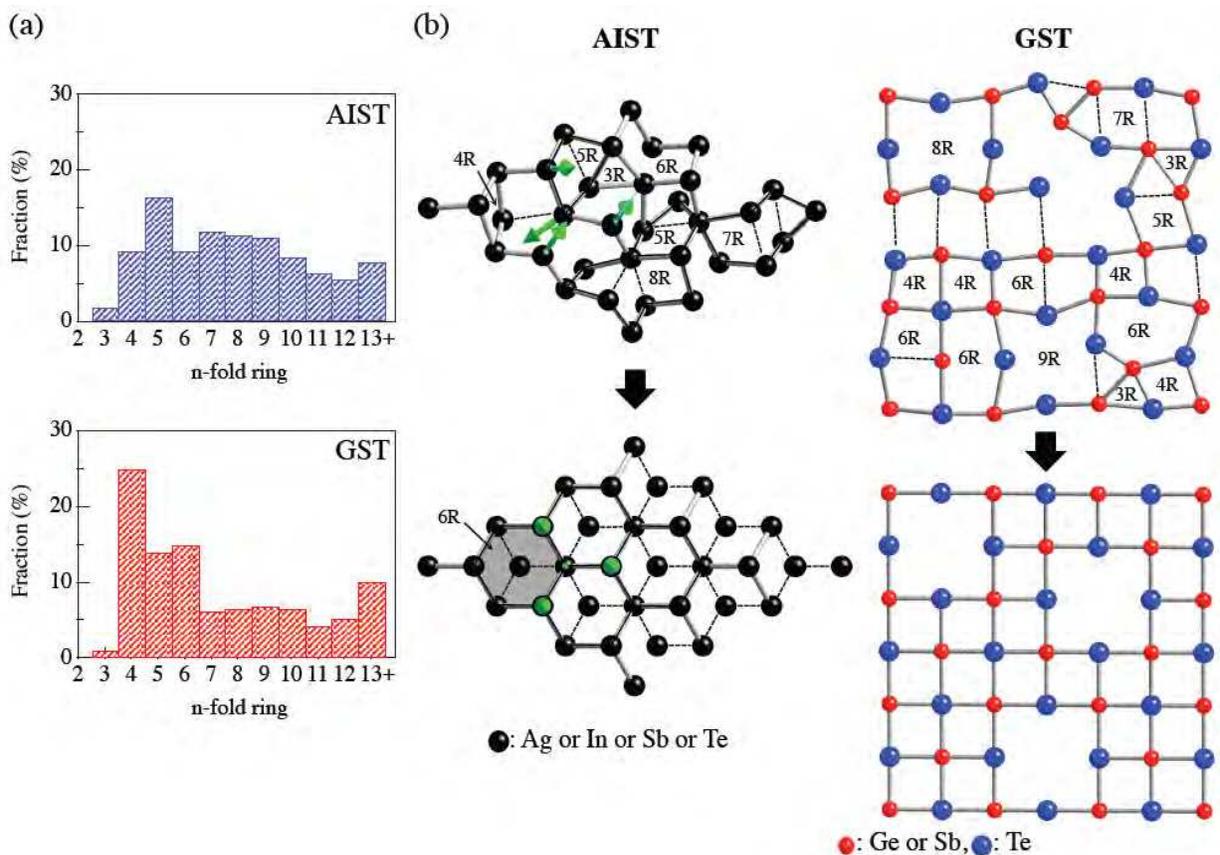

Fig. 16. Ring statistics (a) and possible schemes for fast phase change (b) in a-AIST and a-GST.

5. Conclusion

We described the detail of the X-ray pinpoint structural measurement system for investigation of optical recording process. Furthermore, we showed the recent progress for fully understanding the atomic structure of AIST and compare it to GST with the research combined X-ray diffraction, EXAFS, HXPS measurements and computer simulations. These demonstrated that the time resolved X-ray diffraction technique using SR is very powerful for the structural investigation of crystal growth phenomena.

6. Acknowledgment

7. References

Iwasaki, H.; Ide, Y.; Harigaya, M.; Kageyama, Y. & Fujimura, I. (1992). Completely Erasable Phase Change Optical Disk. *Japanese Journal of Applied Physics,* Vol.31, No.2B, (February 1992), pp.461-465, ISSN 0021-4922

Fukuyama, Y.; Yasuda, N.; Kim, J.; Murayama, H.; Tanaka, Y.; Kimura, S.; Kato, K.; Kohara, S.; Moritomo, Y.; Matsunaga, T.; Kojima, R.; Yamada, N.; Tanaka, H.; Ohshima, T. & Takata, M. (2008a). Time-Resolved Investigation of Nanosecond Crystal Growth in Rapid-Phase-Change Materials: Correlation with the Recording Speed of Digital Versatile Disc Media. *Applied Physics Express,* Vol.1, No.4, (March 2008), pp. 045001-1-3, ISSN 1882-0778

Fukuyama, Y.; Yasuda, N.; Kim, J.; Murayama, H.; Ohshima, T.; Tanaka, Y.; Kimura, S.; Kamioka, H.; Moritomo, Y.; Toriumi, K.; Tanaka, H.; Kato, K.; Ishikawa, T. & Takata, M. (2008b). Ultra-high-precision Time Control System over Any Long Time Delay for Laser Pump and Synchrotron X-ray Probe Experiment. *Review of Scientific Instruments,* Vol.79, No.4, (April 2008), pp. 045107-1-4, ISSN 0034-6748

Fukuyama, Y.; Yasuda, N.; Kamioka, H.; Kim, J.; Shibata, T.; Osawa, H.; Nakagawa, T.; Murayama, H.; Kato, K.; Tanaka, Y.; Kimura, S.; Ohshima, T.; Tanaka, H.; Takata, M. & Moritomo, Y. (2010). Simultaneous Measurements of Picosecond Lattice and Charge Dynamics in Co-Fe Cyanides. *Applied Physics Express,* Vol.3, No.1, (January 2010), pp. 016601-1-3, ISSN 1882-0778

Kimura, S.; Moritomo, Y.; Tanaka, Y.; Tanaka, H.; Toriumi, K.; Kato, K.; Yasuda, N.; Fukuyama, Y.; Kim, J; Murayama, H. & Takata, M. (2006). X-ray Pinpoint Structural Measurement for Nanomaterials and Devices at BL40XU of the SPring-8. *AIP Conference Proceedings,* Vol.879, (2006), pp. 61-66, ISSN 0094-243X

Kohara, S.; Kato, K.; Kimura, S.; Tanaka, H.; Usuki, T.; Suzuya, K.; Tanaka, H.; Moritomo, Y.; Matsunaga, T.; Yamada, N.; Tanaka, Y.; Suematsu, H. & Takata, M. (2006). Structural Basis for the Fast Phase Change of $Ge_2Sb_2Te_5$: Ring Statistics Analogy between the Crystal and Amorphous States. *Applied Physics Letters,* Vol.89, No.20, (November 2006), pp. 021910-1-3, ISSN 0003-6951

Kolobov, A.V.; Fons, P.; Frenkel, A.I.; Ankudinov, A.L.; Tominaga, J. & Uruga, T. (2004). Understanding the Phase-change Mechanism of Rewritable Optical Media. *Nature Materials,* Vol.3, No.10, (October 2004), pp. 703-708, ISSN 1476-1122

Kwon, M.-H.; Lee, B.-S.; Bogle, S.N.; Nittala, L.N.; Bishop, S.G.; Abelson, J.R.; Raoux, S.; Cheong, B.-K. & Kim, K.-B. (2007). Nanometer-scale Order in Amorphous $Ge_2Sb_2Te_5$ Analyzed by Fluctuation Electron Microscopy. *Applied Physics Letters,* Vol.90, No.2, (January 2007), pp. 021923-1-3, ISSN 0003-6951

Lee, B.-S.; Abelson, J.R.; Bishop, S.G.; Kang, D.-H.; Cheong, B.-K. & Kim, K.-B. Investigation of the Optical and Electronic Properties of $Ge_2Sb_2Te_5$ Phase Change Material in Its

Amorphous, Cubic, and Hexagonal Phases. (2005). *Journal of Applied Physics,* Vol.97, No.9, (May 2005), pp. 093509-1-8, ISSN 0021-8979

Matsunaga, T.; Akola, J.; Kohara, S.; Honma, T.; Kobayashi, K.; Ikenaga, E.; Jones, R.O.; Yamada, N.; Takata, M. & Kojima, R. (2011). From local structure to nanosecond recrystallization dynamics in AgInSbTe phase-change materials. *Nature Materials,* Vol.10, No.2, (February 2011), pp. 129-134, ISSN 1476-1122

Naito, M.; Ishimaru, M.; Hirotsu, Y. & Takashima, M. (2004). Local Structure Analysis of Ge-Sb-Te Phase Change Materials using High-resolution Electron Microscopy and Nanobeam diffraction. *Journal of Applied Physics,* Vol.95, No.12, (June 2004), pp. 8130-8135, ISSN 0021-8979

Park, J.; Kim, M.R.; Choi, W.S.; Seo, H. & Yeon, C. (1999). Characterization of Amorphous Phases of $Ge_2Sb_2Te_5$ Phase-change Optical Recording Material on Their Crystallization Behavior. *Japanese Journal of Applied Physics,* Vol.38, No.8B, (August 1999), pp. 4775-4779, ISSN 0021-4922

Tanaka, Y.; Hara, T.; Kitamura, H. & Ishikawa, T. (2000). Timing Control of an Intense Picosecond Pulse Laser to the SPring-8 Synchrotron Radiation Pulses. *Review of Scientific Instruments,* Vol.71, No.3, (March 2000), pp. 1268-1274, ISSN 0034-6748

Tanaka, Y.; Fukuyama, Y.; Yasuda, N.; Kim, J.; Murayama, H.; Kohara, S.; Osawa, H.; Nakagawa, T.; Kimura, S.; Kato, K.; Yoshida, F.; Kamioka, H.; Moritomo, Y.; Matsunaga, T.; Kojima, R.; Yamada, N.; Toriumi, K.; Ohshima, T.; Tanaka, H. & Takata, M. (2009). Development of Picosecond Time-resolved Microbeam X-ray Diffraction Technique for Investigation of Optical Recording Process. *Japanese Journal of Applied Physics,* Vol.48, No.3, (March 2009), pp. 03A001-1-5, ISSN 0021-4922

Tanaka, Y.; Ohshima T.; Fukuyama, Y.; Yasuda, N.; Kim, J.; Osawa, H.; Kimura, S.; Togashi, T.; Hara, T.; Kamioka, H.; Moritomo, T.; Tanaka, H.; Takata, M.; Sengoku, H. & Nonoshita, E. (2010). High-Precision Time Delay Control with Continuous Phase Shifter for Pump-Probe Experiments Using Synchrotron Radiation Pulses. *AIP Conference Proceedings,* Vol.1234, (2010), pp. 951-954, ISSN 0094-243X

Wei, J. & Gan, F. (2003). Theoretical Explanation of Different Crystallization Processes between As-deposited and Melt-quenched Amorphous $Ge_2Sb_2Te_5$ Thin Films. *Thin Solid Films,* Vol.441, No.1-2, (September 2003), pp. 292-297, ISSN 0040-6090

Wuttig, M. & Yamada, N. (2007). Phase-change Materials for Rewriteable Data Storage. *Nature Materials,* Vol.6, No.11, (November 2007), pp. 824-832, ISSN 1476-1122

Yamada, N.; Ohno, E.; Akahira, N.; Nishiuchi, K.; Nagata, K. & Takao, M. (1987). High Speed Overwritable Phase Change Optical Disk Material. *Japanese Journal of Applied Physics,* Vol.26, Supplement 26-4, (1987), pp. 61-66, ISSN 0021-4922

Yamada, N. & Matsunaga, T. (2000). Structure of Laser-crystallized $Ge_2Sb_2+xTe_5$ Sputtered Thin Films for Use in Optical Memory. *Journal of Applied Physics,* Vol.88, No.12, (December 2000), pp. 7020-7028, ISSN 0021-8979

Yasuda, N.; Murayama, H.; Fukuyama, Y.; Kim, J.; Kimura, S.; Toriumi, K.; Tanaka, Y.; Moritomo, Y.; Kuroiwa, Y.; Kato, K.; Tanaka, H & Takata, M. (2009). X-ray Diffractometry for the Structure Determination of a Submicrometre Single Powder Grain. *Journal of Synchrotron Radiation,* Vol.16, No.3, (May 2009), pp. 352-357, ISSN 0909-0495

Yasuda, N.; Fukuyama, Y.; Toriumi, K.; Kimura, S. & Takata, M. (2010). Submicrometer Single Crystal Diffractometry for Highly Accurate Structure Determination. *AIP Conference Proceedings,* Vol.1234, (2010), pp. 147-150, ISSN 0094-243X

Zhou, G.F.; Borg, H.J.; Rijpers, J.C.N.; Lankhorst, M.H.R. & Horikx, J.J.L. (2000). Crystallisation Behaviour of Phase Change Materials: Comparison between Nucleation- and Growth-dominated Crystallisation, *Proceedings of SPIE - The International Society for Optical Engineering,* Vol.4090, (2000), pp. 108-115, ISSN 0277-786X

Materials are important to mankind because of the benefits that can be derived from the manipulation of their properties, for example electrical conductivity, dielectric constant, magnetization, optical transmittance, strength and toughness. Materials science is a broad field and can be considered to be an interdisciplinary area. Included within it are the studies of the structure and properties of any material, the creation of new types of materials, and the manipulation of a material's properties to suit the needs of a specific application. The contributors of the chapters in this book have various areas of expertise. therefore this book is interdisciplinary and is written for readers with backgrounds in physical science. The book consists of fourteen chapters that have been divided into four sections. Section one includes five chapters on advanced materials and processing. Section two includes two chapters on bio-materials which deal with the preparation and modification of new types of bio-materials. Section three consists of three chapters on nanomaterials, specifically the study of carbon nanotubes, nano-machining, and nanoparticles. Section four includes four chapters on optical materials.

INTECH
open science | open minds